Effective field theory for double Higgs production

Giuliano Panico

IFAE, Barcelona

'Gearing up for LHC13' workshop

GGI Firenze – 14 September 2015

Based on A. Azatov, R. Contino, G.P., M. Son, arXiv:1502.00539

Introduction

Why double Higgs production?

Obvious answer:

- ❖ measure the **Higgs trilinear coupling!**

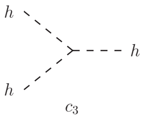

Why double Higgs production?

Obvious answer:

- measure the **Higgs trilinear coupling!**

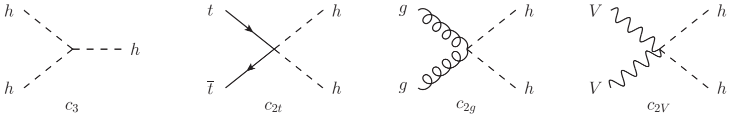

Less obvious answers:

- extract **non-linear couplings** not accessible in single-Higgs measurements (eg. $hh\bar{t}t$, $h^2 G_{\mu\nu} G^{\mu\nu}$ and $h^2 V_\mu V^\mu$)
- improve **single-Higgs measurements** (in particular $\bar{t}th$)
- probe the **strength of EWSB dynamics** at scales $E \gg m_h$

Interpretation strategy

Several new-physics effects can affect double Higgs production

- modifications of Higgs trilinear coupling
- modification of single Higgs couplings
- new non-linear interactions

❖ Corrections to **all** these couplings can arise **simultaneously**

❖ Assuming that only h^3 is modified limits the validity of the fit

Interpretation strategy

Several new-physics effects can affect double Higgs production

- modifications of Higgs trilinear coupling
- modification of single Higgs couplings
- new non-linear interactions

❖ Corrections to **all** these couplings can arise **simultaneously**

❖ Assuming that only h^3 is modified limits the validity of the fit

❖ Proper **interpretation strategy** needed

➢ identify a parametrization of NP effects

➢ perform a global analysis

Note: strategy similar to single Higgs measurements, where distortions of all couplings are taken into account in the fits

The Effective Field Theory approach

- EFT is a perfect framework to analyze the new physics effects below the direct production thresholds of new states
- Useful to obtain a model-independent parametrization in terms of a few local operators
- Many new physics effects grow with energy

$2 \to 2$ processes

$$\frac{\delta \mathcal{A}}{\mathcal{A}} \sim \frac{g_*^2}{g_{\rm SM}^2} \frac{E^2}{m_*^2}$$

m_* scale of NP
g_* coupling of new states

➢ extend the analysis to higher energies to increase the sensitivity

range of validity: $m_h \ll E \ll m_*$

The effective Lagrangian for a Higgs doublet

Assumptions:

- Higgs is an $\mathrm{SU}(2)_L$ doublet
- derivative expansion
- expansion in Higgs powers

$$\mathcal{L} = \mathcal{L}_{SM} + \Delta\mathcal{L}_6 + \Delta\mathcal{L}_8 + \cdots$$

[Buchmuller and Wyler; ... Giudice at al.; Grzadkowski et al.]

$$\Delta\mathcal{L}_6 \supset \frac{\overline{c}_H}{2v^2}[\partial_\mu(H^\dagger H)]^2 + \frac{\overline{c}_u}{v^2} y_u H^\dagger H \overline{q}_L H^c u_R - \frac{\overline{c}_6}{v^2}\frac{m_h^2}{2v^2}(H^\dagger H)^3 + \frac{\overline{c}_g}{m_w^2} g_s^2 H^\dagger H G_{\mu\nu} G^{\mu\nu}$$

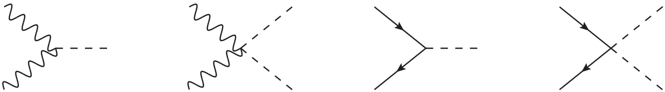

$c_V \simeq 1 - \frac{\overline{c}_H}{2}$ $\quad$ $c_{2V} \simeq 1 - 2\overline{c}_H$ $\quad$ $c_t \simeq 1 - \frac{\overline{c}_H}{2} - \overline{c}_u$ $\quad$ $c_{2t} \simeq -\frac{1}{2}(\overline{c}_H + 3\overline{c}_u)$

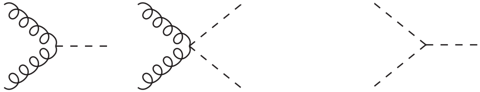

$c_g = c_{2g} = \overline{c}_g \left(\frac{4\pi}{\alpha_2}\right)$ $\quad$ $c_3 \simeq 1 - \frac{3}{2}\overline{c}_H + \overline{c}_6$

The effective Lagrangian for a Higgs doublet

Assumptions:

- Higgs is an $\mathrm{SU}(2)_L$ doublet
- derivative expansion
- expansion in Higgs powers

$$\mathcal{L} = \mathcal{L}_{SM} + \Delta\mathcal{L}_6 + \Delta\mathcal{L}_8 + \cdots$$

[Buchmuller and Wyler; ... Giudice at al.; Grzadkowski et al.]

$$\Delta\mathcal{L}_6 \supset \frac{\bar{c}_H}{2v^2}[\partial_\mu(H^\dagger H)]^2 + \frac{\bar{c}_u}{v^2} y_u H^\dagger H \bar{q}_L H^c u_R - \frac{\bar{c}_6}{v^2}\frac{m_h^2}{2v^2}(H^\dagger H)^3 + \frac{\bar{c}_g}{m_w^2} g_s^2 H^\dagger H G_{\mu\nu} G^{\mu\nu}$$

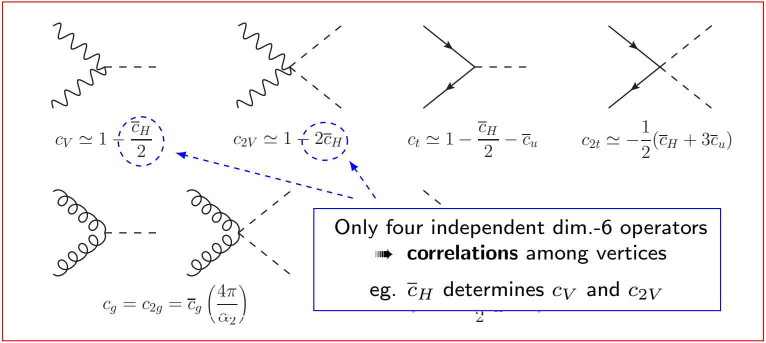

The effective Lagrangian for a Higgs doublet

The effective vertices correspond to the interactions in the unitary gauge

$$\mathcal{L} \supset \left(m_W^2 W_\mu^2 + \frac{m_Z^2}{2} Z_\mu^2\right)\left(1 + 2c_V \frac{h}{v} + c_{2V}\frac{h^2}{v^2}\right) - m_t \bar{t}t \left(1 + c_t \frac{h}{v} + c_{2t}\frac{h^2}{2v^2}\right)$$
$$- c_3 \frac{m_h^2}{2v} h^3 + \frac{g_s^2}{4\pi^2}\left(c_g \frac{h}{v} + c_{2g}\frac{h^2}{2v^2}\right) G_{\mu\nu}^a G^{a\,\mu\nu}$$

This parametrization is more general than the previous one

- valid for a generic Higgs (even not part of a doublet)
- resums the expansion in Higgs powers (if Higgs is a doublet)

Main production channels at hadron colliders

Gluon Fusion

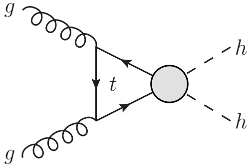

Vector Boson Fusion

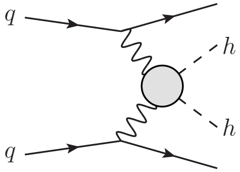

Double Higgs production via Gluon Fusion

results from Azatov, Contino, G.P., Son, arXiv:1502.00539

Double Higgs production via gluon fusion

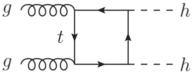

$\sim c_t^2 \times const.$

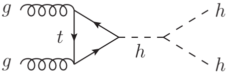

$\sim c_t c_3 \times \frac{m_h^2}{\hat{s}} \log^2\left(\frac{m_t^2}{\hat{s}}\right)$

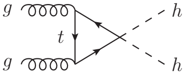

$\sim c_{2t} \times \log^2\left(\frac{m_t^2}{\hat{s}}\right)$

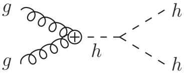

$\sim c_g c_3 \frac{\alpha_s}{4\pi} \times const.$

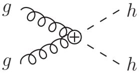

$\sim c_{2g} \frac{\alpha_s}{4\pi} \frac{\hat{s}}{v^2}$

- Different behaviour at high energy $\sqrt{\hat{s}} = m_{hh} \gg 2m_h$
- Dependence on Higgs trilinear suppressed at high energy
  - Events at threshold more sensitive to Higgs trilinear, events at large m_{hh} more important to determine the other operators

Sensitivity to the Higgs trilinear

Dependence on Higgs trilinear c_3
much smaller than on c_t and c_{2t}

[Dib, Rosenfeld, Zerwekh;
Grober and Muhlleitner]

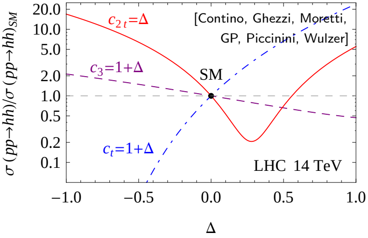

➢ Using the m_{hh} distribution (shape analysis) is essential to disentangle the different new physics effects and maximize sensitivity

The angular distribution

The signal is also characterized by the angle between the Higgs pair and the beam axis in the c.o.m. frame

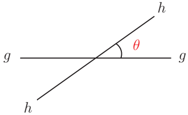

The scattering is mainly due to two partial waves $J_z = 0$ and $J_z = \pm 2$

$$\frac{d\sigma}{d\cos\theta} \sim const. \quad (J_z = 0) \qquad \frac{d\sigma}{d\cos\theta} \sim \sin^2\theta \quad (J_z = \pm 2)$$

- In the SM the $J_z = \pm 2$ amplitude comes only from the box diagram and is extremely suppressed

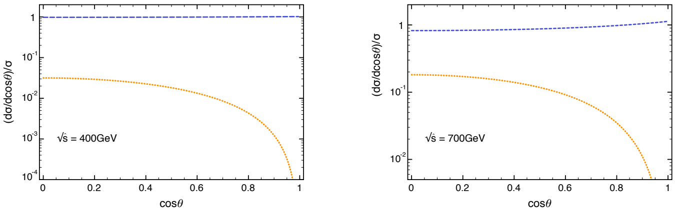

The angular distribution

The signal is also characterized by the angle between the Higgs pair and the beam axis in the c.o.m. frame

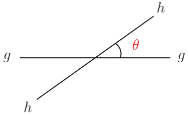

The scattering is mainly due to two partial waves $J_z = 0$ and $J_z = \pm 2$

$$\frac{d\sigma}{d\cos\theta} \sim const. \quad (J_z = 0) \qquad\qquad \frac{d\sigma}{d\cos\theta} \sim \sin^2\theta \quad (J_z = \pm 2)$$

- The BSM diagrams (from dim.-6 operators) only generate contributions with $J_z = 0$

  ➢ the **angular analysis** is **not useful** to disentangle NP effects

  [possible exception: effects from dim.-8 operators (only at $100\ \mathrm{TeV}$)]

The total cross section

Small total production cross section

➢ at LO for the SM

$$\sigma(pp \to hh)_{SM} = 16.2 \text{ fb} \qquad (14 \text{ TeV})$$
$$= 874 \text{ fb} \qquad (100 \text{ TeV})$$

➢ beyond LO computed mainly in the $m_t \to \infty$ approximation

NNLO k-factors: $k_{14 \text{ TeV}} = 2.27$ [De Florian and Mazzitelli]

$k_{100 \text{ TeV}} = 1.75$

$$\sigma(pp \to hh + X)_{SM} = 36.8 \text{ fb} \qquad (14 \text{ TeV})$$
$$= 1.53 \text{ pb} \qquad (100 \text{ TeV})$$

- The $m_t \to \infty$ limit severely distorts the m_{hh} distribution. Conservative estimate of error $\sim 10\%$, can limit ultimate precision.

  (complete m_t dependence at NLO known only for real emission)

Final states

Final states studies so far in the literature:

- $hh \to b\bar{b}\gamma\gamma$: cleanest channel but small cross section

  Baur, Plehn, Rainwater PRD 69 (2004) 053004
  Baglio et al. JHEP 1304 (2013) 151
  Yao arXiv:1308.6302
  Barger et al. PLB 728 (2014) 433
  ATLAS, ATL-PHYS-PUB-2014-019
  Barr et al. arXiv:1412.7154

- $hh \to b\bar{b}\tau\tau$: sizable cross section, promising in the boosted regime

  Baur, Plehn, Rainwater PRD 68 (2003) 033001
  Dolan, Englert, Spannowsky JHEP 1210 (2012) 112
  Baglio et al. JHEP 1304 (2013) 151
  Barr, Dolan, Englert, Spannowsky PLB 728 (2014) 308
  Goertz, Papaefstathiou, Yang, Zurita arXiv:1410.3471

- $hh \to b\bar{b}WW$: large $t\bar{t}$ background, maybe observable in the boosted regime

  Dolan, Englert, Spannowsky JHEP 1210 (2012) 112
  Baglio et al. JHEP 1304 (2013) 151
  Papaefstathiou, Yang, Zurita PRD 87 (2013) 011301

- $hh \to b\bar{b}b\bar{b}$: very difficult, maybe observables in the boosted regime

  de Lima, Papaefstathiou, Spannowsky arXiv:1404.7139

The $b\bar{b}\gamma\gamma$ channel

- Analysis at the $14\ \mathrm{TeV}$ LHC

Highlights of the analysis

Simulations: Parton level + Showering + Hadronization

- Signal at LO rescaled by NNLO k-factor
- Background with MadGraph5

Backgrounds included: $b\bar{b}\gamma\gamma$, $jj\gamma\gamma$ (non resonant)

$b\bar{b}h$, Zh , $t\bar{t}h$ (resonant)

Highlights of the analysis

Simulations: Parton level + Showering + Hadronization

- Signal at LO rescaled by NNLO k-factor
- Background with MadGraph5

Backgrounds included: $b\bar{b}\gamma\gamma$, $jj\gamma\gamma$ (non resonant)

$b\bar{b}h$, Zh, $t\bar{t}h$ (resonant)

$b\bar{b}\gamma\gamma$ has a large NLO k-factor: $k \sim 2$
Mainly due to real emissions

Highlights of the analysis

Simulations: Parton level + Showering + Hadronization

- Signal at LO rescaled by NNLO k-factor
- Background with MadGraph5

Backgrounds included: $b\bar{b}\gamma\gamma\,,\, jj\gamma\gamma$ (non resonant)

$b\bar{b}h\,,\, Zh\,,\, t\bar{t}h$ (resonant)

Selection tags: 2 b-tagged jets + 2 photons

efficiencies: $\epsilon_b = 0.7\,,\quad \epsilon_{j\to b} = 0.01\,,\quad \epsilon_\gamma = 0.8$

Kinematic selection for the $14\ \mathrm{TeV}$ LHC

objects reconstruction: $p_T(j,\gamma) > 25\ \mathrm{GeV}, \quad |\eta(j,\gamma)| < 2.5$

veto isolated leptons: $p_T(l) > 20\ \mathrm{GeV}, \quad |\eta(l)| < 2.5$

first selection: $p_{T>}(b,\gamma) > 50\ \mathrm{GeV}$

$p_{T<}(b,\gamma) > 30\ \mathrm{GeV}$

Kinematic selection for the 14 TeV LHC

objects reconstruction: $p_T(j,\gamma) > 25$ GeV, $|\eta(j,\gamma)| < 2.5$

veto isolated leptons: $p_T(l) > 20$ GeV, $|\eta(l)| < 2.5$

first selection: $p_{T>}(b,\gamma) > 50$ GeV

$p_{T<}(b,\gamma) > 30$ GeV

angular cuts: $\Delta R(b,b) < 2$, $\Delta R(\gamma,\gamma) < 2$, $\Delta R(b,\gamma) > 1.5$

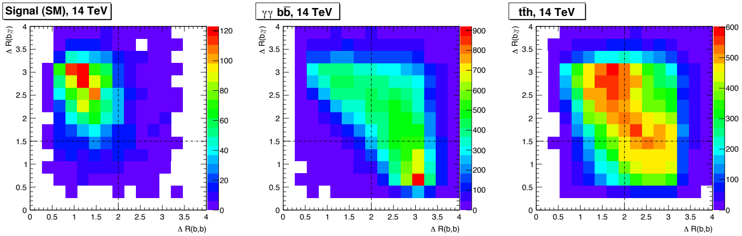

Kinematic selection for the $14\ \mathrm{TeV}$ LHC

objects reconstruction: $p_T(j,\gamma) > 25\ \mathrm{GeV}, \quad |\eta(j,\gamma)| < 2.5$

veto isolated leptons: $p_T(l) > 20\ \mathrm{GeV}, \quad |\eta(l)| < 2.5$

first selection: $p_{T>}(b,\gamma) > 50\ \mathrm{GeV}$

$p_{T<}(b,\gamma) > 30\ \mathrm{GeV}$

angular cuts: $\Delta R(b,b) < 2, \quad \Delta R(\gamma,\gamma) < 2, \quad \Delta R(b,\gamma) > 1.5$

Higgs reconstruction: $105\ \mathrm{GeV} < m_{bb}^{\mathrm{reco}} < 145\ \mathrm{GeV}$

$120\ \mathrm{GeV} < m_{\gamma\gamma}^{\mathrm{reco}} < 130\ \mathrm{GeV}$

Backgrounds and shape analysis

Events in **SM signal** and **backgrounds** with $L = 3\ \mathrm{ab}^{-1}$

	hh	$b\bar{b}\gamma\gamma$	$\gamma\gamma jj$	$t\bar{t}h$	$b\bar{b}h$	Zh
After first selection	28.5	6919	684	130	7.2	24.5
After angular cuts	17.8	1274	104	29	1.2	15.8
After Higgs reco.	12.8	24.2	2.21	9.9	0.40	0.41

➢ dominant background: irreducible $b\bar{b}\gamma\gamma$

Simple **shape analysis** by binning the m_{hh} distribution (in 6 categories)

m_{hh}^{reco} [GeV]	$250-400$	$400-550$	$550-700$	$700-850$	$850-1000$	$1000-$
hh	2.14	6.34	2.86	0.99	0.33	0.17
$\gamma\gamma b\bar{b}$	7.69	10.1	3.35	1.38	1.18	0.59
$\gamma\gamma jj$	0.66	0.95	0.31	0.16	0.08	0.045
$t\bar{t}h$	3.33	4.53	1.41	0.41	0.16	0.043
$b\bar{b}h$	0.20	0.16	0.03	0.0054	0.0022	0.00054
Zh	0.13	0.19	0.067	0.021	0.009	0.0009

Jet and W veto

Only marginal improvement from veto on extra hadronic activity

- Jet veto: $N(jets) < 4$ removes 80% of $t\bar{t}h$, keeps 70% of signal
- W veto: $N(W_{had}) = 0$ removes 50% of $t\bar{t}h$, keeps 90% of signal

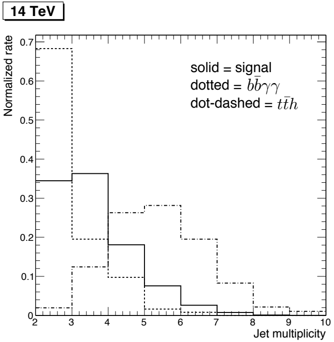

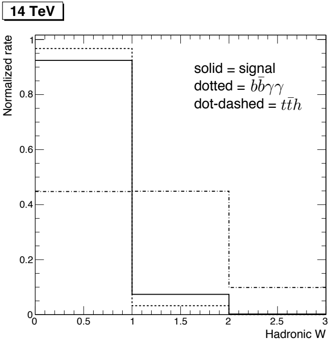

The $b\bar{b}\gamma\gamma$ channel

- Prospects at a future $100\ \mathrm{TeV}$ hadronic collider

Kinematic selection at FCC_{100}

The **angular distributions** at $100\ \mathrm{TeV}$ are similar to the ones at LHC_{14}

- adopt the same angular cuts and Higgs reconstruction windows

$$\Delta R(b,b) < 2, \quad \Delta R(\gamma,\gamma) < 2, \quad \Delta R(b,\gamma) > 1.5$$

$$105\ \mathrm{GeV} < m_{bb}^{\mathrm{reco}} < 145\ \mathrm{GeV}$$

$$120\ \mathrm{GeV} < m_{\gamma\gamma}^{\mathrm{reco}} < 130\ \mathrm{GeV}$$

- slightly tighter p_T cuts

$$p_{T>}(b,\gamma) > 60\ \mathrm{GeV}\,, \qquad p_{T<}(b,\gamma) > 40\ \mathrm{GeV}$$

Main features at 100 TeV: Backgrounds

Three **main differences** between 14 TeV and 100 TeV:

1. Change in the **background** composition

Number of events with $L = 3\ \mathrm{ab}^{-1}$	hh	$b\bar{b}\gamma\gamma$	$t\bar{t}h$	$\gamma\gamma jj$	$b\bar{b}h$	Zh
14 TeV	12.8	24.2	9.9	2.21	0.40	0.41
100 TeV	303	137	303	18.2	6.2	3.2

- main background at LHC_{14}: $b\bar{b}\gamma\gamma$
- main background at FCC_{100}: $t\bar{t}h$

Main features at 100 TeV: Backgrounds

Three **main differences** between 14 TeV and 100 TeV:

1. Change in the **background** composition

Number of events with $L = 3\ \mathrm{ab}^{-1}$

	hh	$b\bar{b}\gamma\gamma$	$t\bar{t}h$	$\gamma\gamma jj$	$b\bar{b}h$	Zh
14 TeV	12.8	24.2	9.9	2.21	0.40	0.41
100 TeV	303	137	303	18.2	6.2	3.2

- main background at LHC_{14}: $b\bar{b}\gamma\gamma$
- main background at FCC_{100}: $t\bar{t}h$

➢ **Jet-veto** or **W-veto** useful to reduce the $t\bar{t}h$ background at FCC_{100}

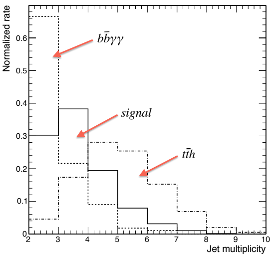

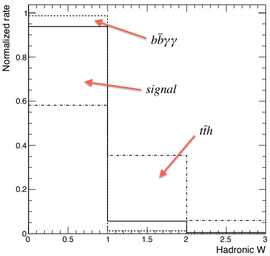

Main features at 100 TeV: Kinematics of the signal

2. Larger boost of the hh system ➠ higher fraction of decay products outside the detector region

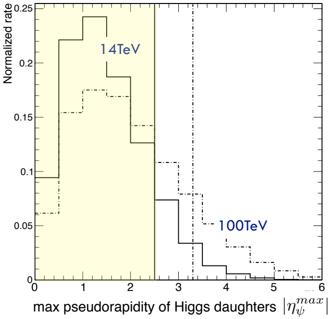

- Fraction of events with $|\eta| > 2.5$: 13% at LHC ➠ 30% at 100 TeV
- Need to extend to $|\eta| \leq 3.3$ to keep same fraction of events

Main features at 100 TeV: Kinematics of the signal

3. **Larger invariant mass** of the hh system

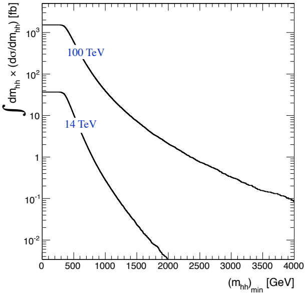

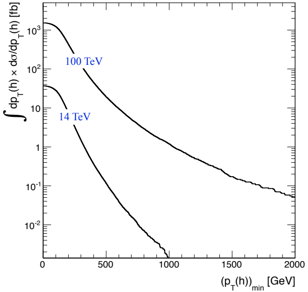

Highest accessible m_{hh} and p_T estimated by requiring at least 5 events beyond the threshold

channel	$b\bar{b}b\bar{b}$ (33.3%)	$b\bar{b}WW^*$ (24.9%)	$b\bar{b}\tau^+\tau^-$ (7.35%)	$b\bar{b}\gamma\gamma$ (0.264%)
Cross section	> 0.05 fb	> 0.067 fb	> 0.227 fb	> 6.31 fb
m_{hh} [GeV]	$< 1340(4290)$	< 1280 (4170)	< 1039 (3235)	< 558 (1552)
p_T [GeV]	$< 575(2000)$	< 575 (2000)	< 550 (1890)	< 210 (664)

[We use $L = 3/\text{ab}$ and assume 10% efficiency. Numbers in parenthesis for a 100 TeV collider]

Main features at 100 TeV: Kinematics of the signal

3. Larger invariant mass of the hh system

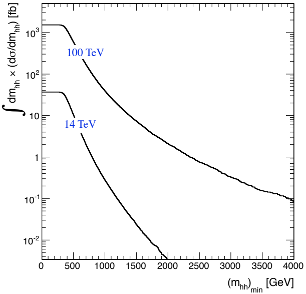

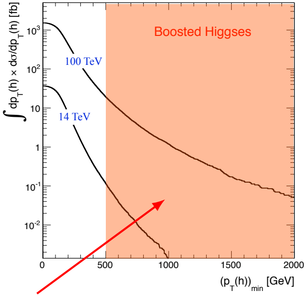

H ... least 5 events
be ...

Jet substructure techniques crucial at 100 TeV

$$\Delta R \sim \frac{2m_h}{p_T(h)} \lesssim 0.5 \quad \text{for} \quad p_T(h) \gtrsim 500 \text{ GeV}$$

c...			)	$b\bar{b}\gamma\gamma$ (0.264%)
Cross section	> 0.05 fb	> 0.067 fb	> 0.227 fb	> 6.31 fb
m_{hh} [GeV]	$< 1340(4290)$	$< 1280\ (4170)$	$< 1039\ (3235)$	$< 558\ (1552)$
p_T [GeV]	$< 575(2000)$	$< 575\ (2000)$	$< 550\ (1890)$	$< 210\ (664)$

[We use $L = 3/\text{ab}$ and assume 10% efficiency. Numbers in parenthesis for a 100 TeV collider]

The $b\bar{b}\gamma\gamma$ channel

- Sensitivity on the EFT coefficients

Sensitivity on the EFT coefficients

We consider three benchmark scenarios

	LHC_{14}	HL-LHC	FCC_{100}
$\sqrt{s}$	14 TeV	14 TeV	100 TeV
Luminosity	$L = 300\ \mathrm{fb}^{-1}$	$L = 3\ \mathrm{ab}^{-1}$	$L = 3\ \mathrm{ab}^{-1}$

- Bayesian analysis for parameters of interest, marginalizing or fixing the others
- Flat prior for unconstrained EFT coefficients
- Gaussian constraints from single-Higgs data (we use ATLAS projections [ATL-PHYS-PUB-2013-014])
- No theoretical uncertainties or systematic error included

Sensitivity on the EFT coefficients

Precision on single-Higgs observables from ATLAS projection

[ATL-PHYS-PUB-2013-014]

	$300\ \text{fb}^{-1}$	$3\ \text{ab}^{-1}$
$\sigma(\bar{c}_H)$	7.9%	5.4%
$\sigma(\bar{c}_u)$	5.9% $(w/t\bar{t}h)$	5.4% $(w/t\bar{t}h)$
	20% $(t\bar{t}h)$	7.7% $(t\bar{t}h)$
$\sigma(\bar{c}_d)$	6.3%	4.4%

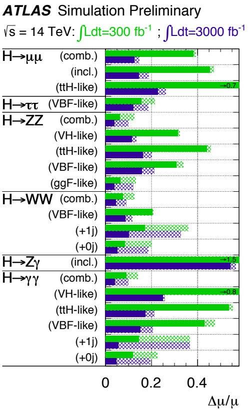

Precision on c_3, c_{2t} and c_{2g}

The non-linear Higgs couplings c_3, c_{2t}, c_{2g} can only be directly accessed in double Higgs production

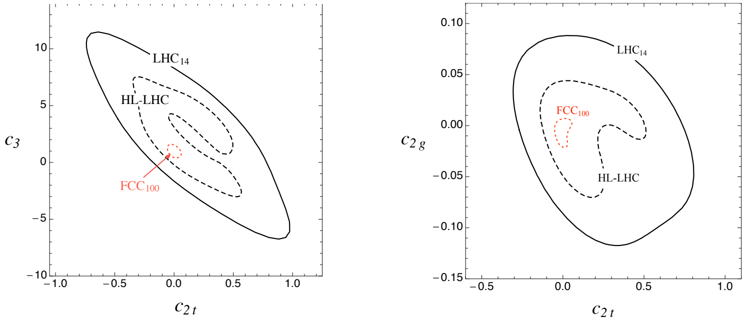

- Higgs trilinear c_3 can only be extracted at FCC (at LHC only $\mathcal{O}(1)$ determination)
- good precision on c_{2t} and c_{2g}

Exclusive vs inclusive analysis

- Modest improvement from **exclusive analysis** at the LHC
  (small number of signal events hinders shape analysis)

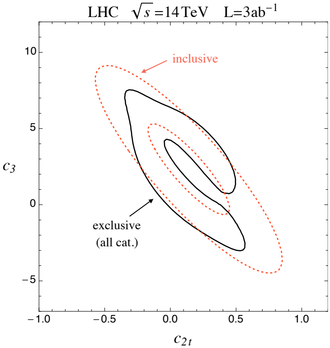

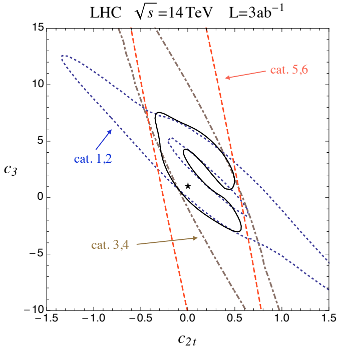

category	1	2	3	4	5	6
m_{hh} [GeV]	$250-400$	$400-550$	$550-700$	$700-850$	$850-1000$	$1000-$

Exclusive vs inclusive analysis

❖ **Exclusive analysis** is crucial at FCC_{100}!

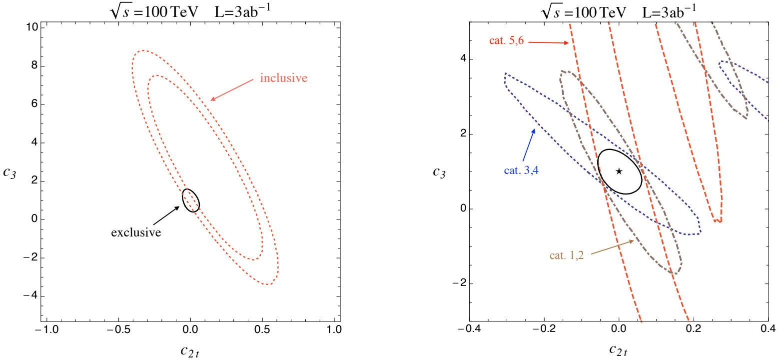

category	1	2	3	4	5	6
m_{hh} [GeV]	250 − 400	400 − 550	550 − 700	700 − 850	850 − 1000	1000 −

Improvement from jet substructure

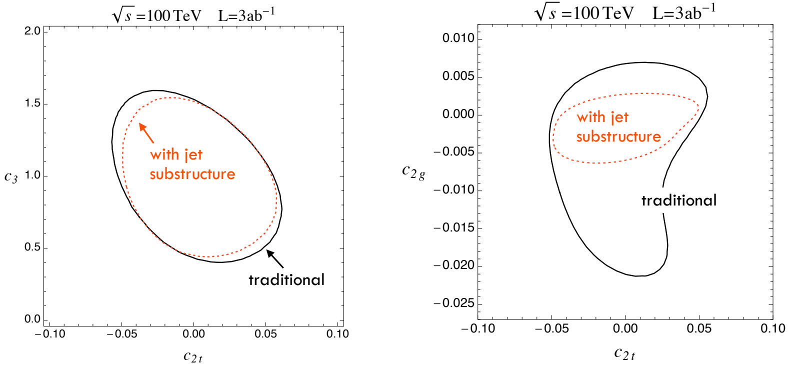

Jet substructure techniques efficiently improve the sensitivity to boosted events at FCC_{100}

- important to extract c_{2g} (effects in the tail of the distribution)
- not crucial to determine c_3 and c_{2t} (effects close to threshold)

Constraining the dim.-6 operators: $\bar{c}_u$ and $\bar{c}_g$

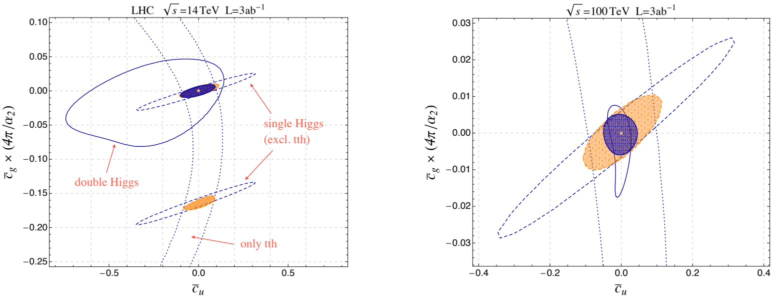

➢ double Higgs can resolve the degeneracy in c_g

➢ at FCC$_{100}$ it can be competitive with $t\bar{t}h$ for the determination of the top Yukawa $\bar{c}_u$ (if precision from single Higgs similar to the LHC one)

Orange region: single Higgs incl. $t\bar{t}h$

Blue region: single + double Higgs

Constraining the dim.-6 operators: $\overline{c}_u$ and $\overline{c}_6$

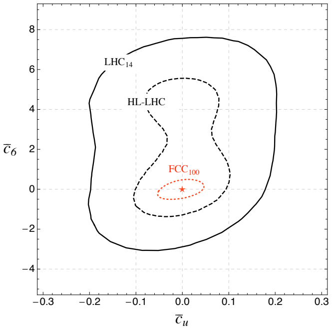

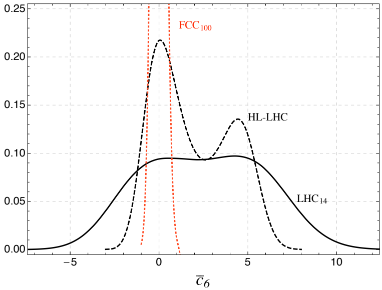

68% probability intervals on $\overline{c}_6$

LHC_{14}	HL-LHC	FCC_{100}
$[-1.2, 6.1]$	$[-1.0, 1.8] \cup [3.5, 5.1]$	$[-0.33, 0.29]$

The statistical treatment

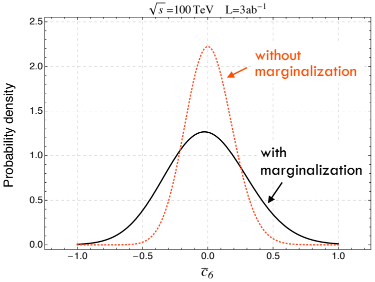

Marginalization has a significant impact on the precision on $\overline{c}_6$

	with marginalization	without marginalization
precision at FCC_{100}	$[-0.33, 0.29]$	$[-0.18, 0.18]$

The statistical treatment

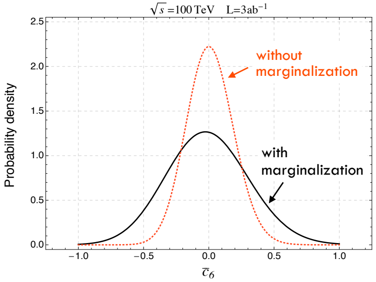

Marginalization has a significant impact on the precision on $\bar{c}_6$

	with marginalization	without marginalization
precision at FCC_{100}	$[-0.33, 0.29]$	$[-0.18, 0.18]$

e.g. uncertainty on $\bar{c}_u$ increases uncertainty on $\bar{c}_6$

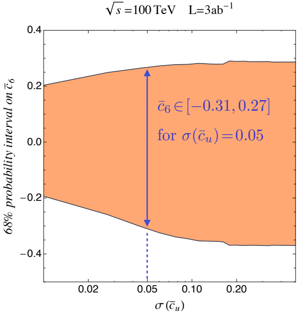

Projections by the experimental collaborations

[CMS CR -2015/044]

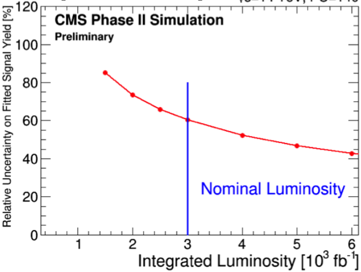

[ATL-PHYS-PUB-2014-019]

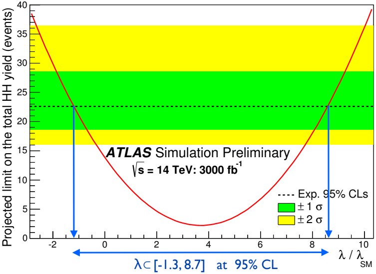

The projections from the experimental collaborations confirm that the Higgs trilinear coupling can only be measured at $\mathcal{O}(1)$ at the LHC

Double Higgs via Vector Boson Fusion

results from Contino, Rojo, work in progress (courtesy of R. Contino)

Double Higgs production via vector boson fusion

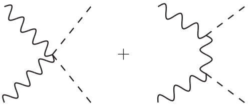

$\sim \frac{\hat{s}}{v^2}(c_V^2 - c_{2V})$

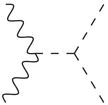

$\sim \frac{m_h^2}{v^2} c_3 c_V$

- Sensitivity on c_3 mainly from events at threshold
- Events with large m_{hh} more important to extract c_{2V}

Study of double Higgs in VBF at 100 TeV requires a detector in the very forward region

$\sim 67\%$ of signal events has $|\eta(j)_{max}| > 4.5$

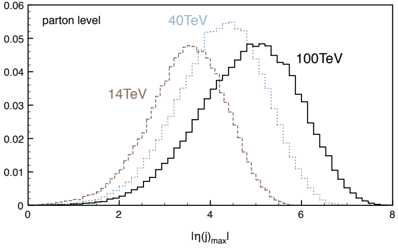

Higgs couplings from the $hh \to 4b$ channel

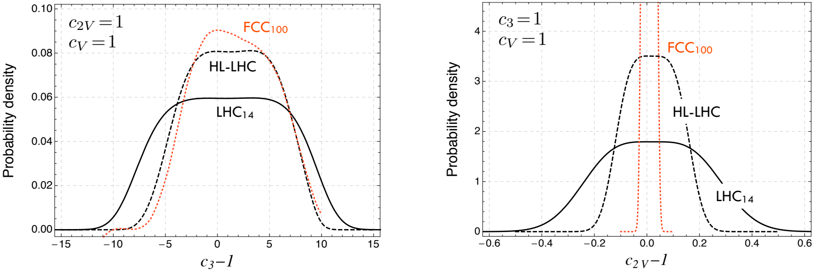

Huge background, sensitive only if deviations much larger than the SM

- Poor precision on Higgs trilinear (not competitive with gluon fusion)
- FCC_{100} can provide good bounds on $\Delta c_{2V} \equiv c_{2V} - 1$

68% probability intervals on Δc_{2V}	LHC_{14}	HL-LHC	FCC_{100}
	$[-0.18, 0.22]$	$[-0.08, 0.12]$	$[-0.01, 0.03]$

Conclusions

Conclusions

❖ Double Higgs production is an essential channel to extract information on the Higgs non-linear couplings

- Measure te Higgs trilinear coupling c_3
- Access new couplings to top and vector bosons: c_{2t}, c_{2g}, c_{2V}.
- Global analysis needed to get a model-independent fit

❖ **Main processes** at hadronic colliders:

I. **Gluon Fusion** (in particular $gg \to hh \to b\bar{b}\gamma\gamma$)

- Higgs trilinear coupling c_3

$$\delta\lambda \sim \mathcal{O}(1) \;\; @\, \mathrm{HL-LHC} \qquad\qquad \delta\lambda \sim 30\% \;\; @\, \mathrm{FCC}$$

- coupling to tops c_{2t} and gluons c_{2g}
- at FCC_{100} possible relevance to measure top Yukawa

II. **Vector Boson Fusion**

- coupling to EW bosons c_{2V}

Backup material

Leptonic machines: Main production channels

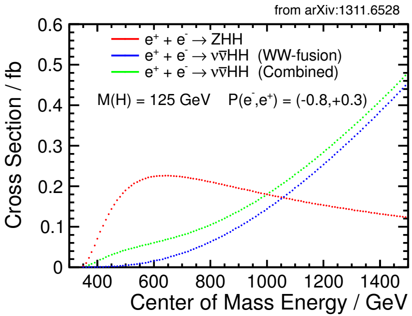

Leptonic machines: Main production channels

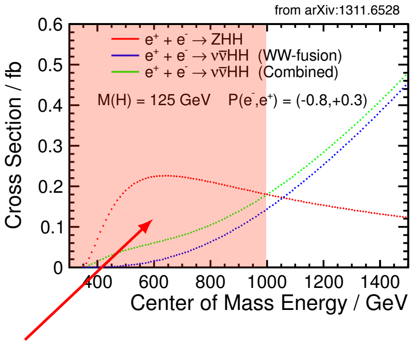

Double Higgs-strahlung (DHS)

dominant below 1 TeV

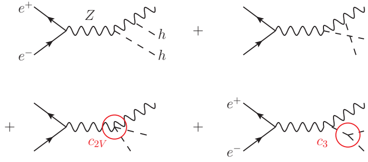

Leptonic machines: Main production channels

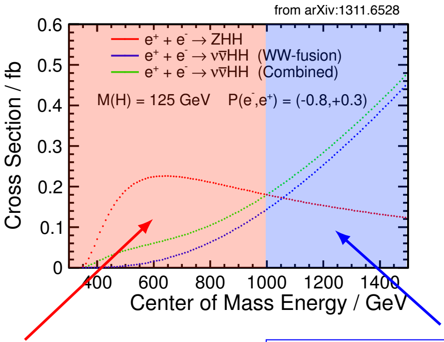

Double Higgs-strahlung (DHS)

dominant below 1 TeV

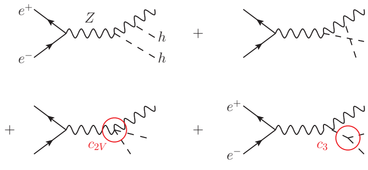

Vector Boson Fusion (VBF)

dominant above 1 TeV

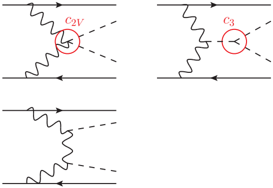

Leptonic machines: Expected precision on c_3 and c_{2V}

	COM Energy	Precision	Process	Reference
ILC	500 GeV $[L = 500\ \text{fb}^{-1}]$	$\Delta c_3 \sim 104\%$	DHS	ILC TDR, Volume 2, arXiv:1306.6352
	1 TeV $[L = 1\ \text{ab}^{-1}]$	$\Delta c_3 \sim 28\%$	VBF	ILC TDR, Volume 2, arXiv:1306.6352
		$\Delta c_{2V} \sim 20\%$	DHS	Contino et al., JHEP 1402 (2014) 006
CLIC	1.4 TeV $[L = 1.5\ \text{ab}^{-1}]$	$\Delta c_3 \sim 24\%$	VBF	Roloff (CLICdp Coll.), talk at LCWS14
		$\Delta c_{2V} \sim 7\%$		
	3 TeV $[L = 2\ \text{ab}^{-1}]$	$\Delta c_3 \sim 12\%$		
		$\Delta c_{2V} \sim 3\%$		

Leptonic machines: Expected precision on c_3 and c_{2V}

	COM Energy	Precision	Process	Reference
ILC	500 GeV $[L = 500\ \mathrm{fb}^{-1}]$	$\Delta c_3 \sim 104\%$	DHS	ILC TDR, Volume 2, arXiv:1306.6352
	1 TeV $[L = 1\ \mathrm{ab}^{-1}]$	$\Delta c_3 \sim 28\%$	VBF	ILC TDR, Volume 2, arXiv:1306.6352
		$\Delta c_{2V} \sim 20\%$	DHS	Contino et al., JHEP 1402 (2014) 006
CLIC	1.4 TeV $[L = 1.5\ \mathrm{ab}^{-1}]$	$\Delta c_3 \sim 24\%$	VBF	Roloff (CLICdp Coll.), talk at LCWS14
		$\Delta c_{2V} \sim 7\%$		
	3 TeV $[L = 2\ \mathrm{ab}^{-1}]$	$\Delta c_3 \sim 12\%$		
		$\Delta c_{2V} \sim 3\%$		

Precision on Higgs trilinear slightly better than FCC_{100} (effects at threshold)

Leptonic machines: Expected precision on c_3 and c_{2V}

	COM Energy	Precision	Process	Reference
ILC	500 GeV $[L = 500\ \mathrm{fb}^{-1}]$	$\Delta c_3 \sim 104\%$	DHS	ILC TDR, Volume 2, arXiv:1306.6352
	1 TeV $[L = 1\ \mathrm{ab}^{-1}]$	$\Delta c_3 \sim 28\%$	VBF	ILC TDR, Volume 2, arXiv:1306.6352
		$\Delta c_{2V} \sim 20\%$	DHS	Contino et al., JHEP 1402 (2014) 006
CLIC	1.4 TeV $[L = 1.5\ \mathrm{ab}^{-1}]$	$\Delta c_3 \sim 24\%$	VBF	Roloff (CLICdp Coll.), talk at LCWS14
		$\Delta c_{2V} \sim 7\%$		
	3 TeV $[L = 2\ \mathrm{ab}^{-1}]$	$\Delta c_3 \sim 12\%$		
		$\Delta c_{2V} \sim 3\%$		

Precision on c_{2V} worse than FCC_{100}
(effects grow with energy)